

DONOD: Robust and Generalizable Instruction Fine-Tuning for LLMs via Model-Intrinsic Dataset Pruning

Jucheng Hu
 Shanghai Artificial Intelligence Laboratory
 University College London
 jucheng.hu.20@ucl.ac.uk

Surong Yang
 Shanghai Artificial Intelligence Laboratory
 Nanjing University
 sryang@smail.nju.edu.cn

Dongzhan Zhou* & Lijun Wu
 Shanghai Artificial Intelligence Laboratory
 {zhoudongzhan, wulijun}@pjlab.org.cn

arXiv:2504.14810v1 [cs.AI] 21 Apr 2025

Abstract

Ad-hoc instruction fine-tuning of large language models (LLMs) is widely adopted for domain-specific adaptation. While domain-specific supervised fine-tuning (SFT) is effective and efficient, it often weakens cross-domain generalization and struggles with noisy training data. To address these challenges, we propose DONOD, a lightweight model-intrinsic data pruning method. Our approach evaluates data using two model-parameter-based metrics: Delta of Norm (DON), which captures the cumulative influence on model weights, and Norm of Delta (NOD), which quantifies weight instability. Moreover, by employing the Technique for Order of Preference by Similarity to Ideal Solution (TOPSIS) algorithm, we effectively filter noisy, unlearnable, and generalization-harming samples without relying on auxiliary models during the SFT process. Experiments on mathematical tasks demonstrate that data selected by DONOD achieve superior fine-tuning efficiency and improved robustness against noisy data. By filtering out 70% of the full dataset, we improve target-domain accuracy by 14.90% and cross-domain accuracy by 5.67%. Meanwhile, our selected data present superior cross-architecture generalization. Data pruned by smaller models (e.g., Llama 3.1-8B) generalize effectively on larger models (e.g., Llama 2-13B). Compared to existing related methodologies, DONOD demonstrates comparable or superior performance while remaining dataset-agnostic, enabling broader applicability.

1 Introduction

Large language models (LLMs) have revolutionized natural language processing, but their effective adaptation to domain-specific tasks remains challenging. Supervised fine-tuning (SFT) is a widely adopted approach for tailoring LLMs to specialized applications. However, it faces critical limitations: overfitting to narrow domains, degradation in cross-domain performance, and sensitivity to noisy or low-quality training data. These issues stem from the inherent trade-off between domain-specific adaptation and generalization, exacerbated by the reliance of existing methods on auxiliary

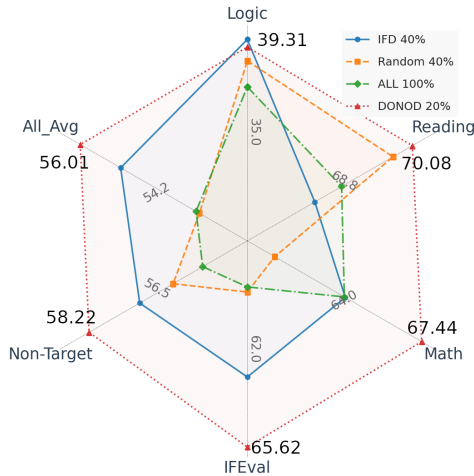


Figure 1: Overview performance of our proposed DONOD. Result obtained on the same setting used in § 4.3

*Corresponding author

ry models or predefined validation sets for data selection.

Traditional ad-hoc SFT methods often prioritize domain-specific performance, leading to catastrophic forgetting, where the model loses capabilities in non-target domains. While efforts to mitigate this include dataset curation or mixing diverse data, these approaches either incur high costs or fail to address noise-induced instability. Recent advances in data pruning, such as reward model-guided selection or gradient-based methods, introduce computational overhead or require access to target validation sets, limiting their practicality in real-world scenarios.

To address the issues above, we propose DONOD, a model-intrinsic dataset pruning framework that jointly optimizes for learning efficacy and generalization preservation. DONOD leverages two complementary metrics derived from the model’s weight dynamics. **Delta of Norm (DON)** captures the cumulative shift in model weight magnitudes during training, acting as a proxy for generalization by favoring samples that stabilize parameter norms. **Norm of Delta (NOD)**: Quantifies the instability caused by individual samples, filtering out noisy or unlearnable data by identifying abrupt weight changes. These metrics are integrated via the Technique for Order of Preference by Similarity to Ideal Solution (TOPSIS) algorithm, which systematically balances the competing goals of maximizing generalization via DON and minimizing harmful updates via NOD. Crucially, DONOD operates without auxiliary models or validation sets, relying solely on the model’s intrinsic training dynamics, thereby ensuring high efficiency.

Experimental evaluations on mathematical reasoning and logical reasoning tasks demonstrate DONOD’s efficacy: pruning 70% of the full dataset improves target-domain accuracy by 14.90% and cross-domain accuracy by 5.67% compared to standard SFT. Notably, datasets pruned by smaller models (e.g., Llama 3.1-8B) generalize effectively to larger architectures (e.g., Llama 2-13B), showcasing strong cross-architecture robustness. DONOD outperforms existing state-of-the-art methods, achieving superior performance with fewer samples while maintaining dataset-agnostic flexibility.

We summarize our contribution as follows: (1) We propose a novel framework for model-intrinsic dataset pruning that unifies generalization and noise filtering through weight-norm analysis. (2) We design a scalable implementation focusing on output-layer weight dynamics, reducing computational overhead while preserving signal fidelity. (3) Empirical validation of cross-domain and cross-architecture generalization demonstrates DONOD’s broad applicability in real-world SFT scenarios.

2 Related Work

Dataset pruning for LLM SFT critically impacts model performance. Traditional methods often rely on external models as quality judges (Du et al. (2023), Chen et al. (2024)) or employ reward models to identify high-quality data. However, this dependence on auxiliary models—whether trained from scratch or repurposed—incurs significant computational costs and limits scalability. Recent studies (Li et al. (2025)) further question the effectiveness of this paradigm.

Alternative approaches focus on intrinsic data metrics. For instance, Cao et al. (2024) proposes evaluating data quality through features like length, naturalness, and coherence. However, the field lacks consensus on universal metrics: while Chen et al. (2023) emphasizes diversity, Liu et al. (2024) argues for prioritizing complex or challenging samples. This ambiguity motivates the third category—model-intrinsic methods—which leverage the model’s own training dynamics to bypass explicit metric definitions. As noted by Jiang et al. (2019), the model’s response to data inherently signals its utility for learning, enabling automated dataset pruning.

Model-intrinsic pruning methods bifurcate based on scenarios. The first category assumes access to a target data distribution, often via validation or development sets. For example, Mindermann et al. (2022) approximates loss differences between holdout and training sets, while Xia et al. (2024) uses gradient similarity between validation and training data. These methods falter when target distributions are ambiguous or undefined—common in scenarios aiming to enhance broad capabilities rather than optimize for specific benchmarks.

The second category eliminates reliance on target distributions. Works like Wang et al. (2024), Jiang et al. (2019), Loshchilov & Hutter (2016), and Li et al. (2024) employ loss or perplexity thresholds, assuming high-loss samples are valuable learning challenges. However, this assumption proves brittle for noisy or mislabeled data, where high loss reflects annotation errors rather than learnable patterns.

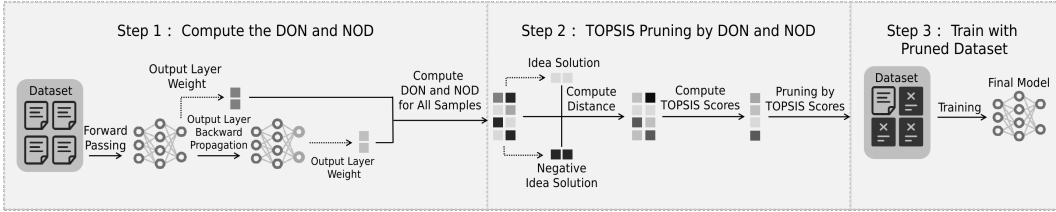


Figure 2: Overview of our proposed DONNOD, which follows a lightweight, three-step pipeline: (1) Compute DON and NOD metrics for each sample, (2) Apply TOPSIS pruning to filter harmful/low-quality data, and (3) Train the model on the pruned dataset.

Furthermore, excessively difficult samples may exceed the model’s current capacity, rendering them unproductive for training.

Both categories neglect cross-domain generalization. Methods targeting specific distributions risk catastrophic forgetting, where performance gains on target tasks degrade generalizability. Conversely, loss-based selection exacerbates this by prioritizing samples that induce large weight updates, destabilizing pre-trained knowledge.

To address these limitations, we propose DONOD. DON functions as a proxy of generalization, while NOD recognizes that the sample causes significant instability in the model weight. Integrated via the TOPSIS, DONOD filter noisy, unlearnable, and generalization-harming samples without auxiliary models or predefined targets.

3 Methodology

3.1 Overview

DONOD begins with a critical observation regarding ad-hoc instruction fine-tuning (SFT) for large language models (LLMs). Traditional SFT methods are highly data-dependent, and using a narrowly focused dataset can lead to catastrophic forgetting, which leads to performance degradation in non-target domains during specialization. For instance, fine-tuning on mathematical tasks may significantly impair the model’s ability in reading comprehension. While mixing diverse data can mitigate this issue, it introduces additional training costs and issues of domain proportion balance. Furthermore, the quality of individual samples significantly impacts fine-tuning efficacy, yet identifying high-quality data remains an open problem.

To address these issues, DONOD introduces a data-efficient alternative: instead of augmenting datasets, we prune harmful or low-quality samples that impede generalization. Our approach is grounded in a key insight: the Frobenius norm of weight changes (before vs. after fine-tuning) can estimate each sample’s impact. Specifically, DONOD consists of three core components: 1). DON and NOD. These metrics quantify a sample’s tendency to exacerbate overfitting or catastrophic forgetting. 2). TOPSIS Pruning: Samples are ranked and selected based on DON and NOD, retaining only high-quality data that balances task-specific improvement and cross-domain generalization. 3). Proxy-Based Scalability: We focus on output-layer weight changes as a proxy for full-model behavior, significantly reducing overhead without sacrificing efficacy.

3.2 Theoretical Foundations

3.2.1 Choice of Frobenius Norm

The Frobenius norm is a matrix norm defined for a matrix $W \in \mathbb{R}^{m \times n}$ as the square root of the sum of the squares of its elements, i.e., $\|W\|_F = \sqrt{\sum_{i=1}^m \sum_{j=1}^n |w_{i,j}|^2}$. Compared to other norms, it offers specific advantages. For instance, the ℓ_1 norm is given by $\|W\|_1 = \sum_{i=1}^m \sum_{j=1}^n |w_{i,j}|$, it treats the matrix as a flattened vector and measures the total absolute deviation. The ℓ_1 norm’s robustness to outliers makes it suitable for measuring aggregate influence. However, it lacks sensitivity to the fine-grained linear transformation differences represented by the weight matrix, which is critical for data pruning. Moreover, it provides a less effective measure of the magnitude difference for

fine-grained data pruning. To capture the slightest difference between samples, the Frobenius norm shows better performance. In terms of the ℓ_2 norm, for a matrix, it typically implies the Spectral norm and is given by $\|W\|_2 = \sigma_{\max}(W)$, where $\sigma_{\max}(W)$ is the maximum singular value obtained from the singular value decomposition (SVD) of W . This makes the ℓ_2 norm solely focus on the largest singular value, capturing the dominant direction of the matrix’s transformation but ignoring the contribution of smaller singular values. This ignorance of finer structural changes in the weight matrix, making it less suitable for detecting sample-wise influences. Furthermore, the computation of SVD for a large matrix, which is a common situation for modern LLMs, can be a heavy workload, hindering the scalability of the method. For the same matrix $W \in \mathbb{R}^{m \times n}$, comparing with the expensive computation of ℓ_2 spectral norm ($O(\min(mn^2, m^2n))$), Frobenius norm is much more efficient and only requiring $O(mn)$.

3.2.2 DON and NOD Metrics

Let D denote an ad-hoc dataset for instruction fine-tuning, for a specific data sample $D_i \in D$, let $\{W^l\}_1^L$ represent the weight of the model before fine-tuning and $\{W'^l\}_1^L$ the weight matrix after fine-tuning on D_i . We employ the DON_{total} and NOD_{total} to quantify this change. Specifically:

$$DON_{total} = \sum_{l=1}^L (\|W^l\|_F - \|W'^l\|_F) = \sum_{l=1}^L \left(\sqrt{\sum_{i=1}^{m_l} \sum_{j=1}^{n_l} |w_{i,j}^l|^2} - \sqrt{\sum_{i=1}^{m_l} \sum_{j=1}^{n_l} |w'_{i,j}{}^l|^2} \right), \quad (1)$$

where m_l and n_l are the dimensions of the weight matrix mW^l of layer l . Meanwhile, the NOD is defined as:

$$NOD_{total} = \sum_{l=1}^L \|W^l - W'^l\|_F = \sum_{l=1}^L \sqrt{\sum_{i=1}^{m_l} \sum_{j=1}^{n_l} \|w_{i,j}^l - w'_{i,j}{}^l\|^2}. \quad (2)$$

DON_{total} captures the cumulative shift in the model’s weight magnitude, while NOD_{total} measures the direct geometric displacement of weights in parameter space at the current step. These metrics are complementary: DON_{total} reflects the overall scaling of weights, whereas NOD_{total} reflects the sensitivity of model weight on a single sample.

3.2.3 Intuition Behind DON and NOD Metrics

DON as a Proxy for Generalization: A negative DON indicates that fine-tuning on D_i increases the model’s weight magnitude. Works from Bartlett (1996) and Yin et al. (2020) show that under certain constraints, smaller norms of weight enable better generalization from the perspective of statistical learning theory. This is also supported by the study of Shalev-Shwartz & Ben-David (2014), its increment relates to the regularization principles, where smaller norms often correlate with lower generalization error (e.g., weight decay). Intuitively, samples that induce a significant increase in the Frobenius norm contribute to the complexity of the model, potentially damage its ability to generalize across domains, and high and positive DON indicate the simplification of the model and better generalization. Our experimental results support this intuition, showing that samples yielding high DON positive values improve cross-domain accuracy.

NOD as an Indicator of Bad Sample: A high NOD value indicates that the data point D_i has a significant influence on the model. In the context of ad-hoc SFT, training begins with a model that already possesses a certain level of generalization. Since the model is unlikely to encounter entirely new information or learn fundamentally new concepts after pretraining, data points with high NOD values are often indicative of low-quality samples, such as mislabeled or noisy data. To address this, our method focuses on filtering out samples with high NOD values, thereby removing noisy or unlearnable data from the training process.

3.3 Implementation Details

3.3.1 Focus on Output Layer Weights

While the Frobenius norm can be applied to all model weights, we restrict the use of the weight to the output layer. Prior works (Nadipalli (2025) and Rosati et al. (2024)) have shown that fine-tuning primarily affects later layers, with the output layer acting as a bottleneck for domain adaptation. This restriction benefits in two critical ways: 1). Computational Efficiency: The output layer is typically smaller than the hidden layers, reducing the computational cost of computing norms across iterations, 2). Interpretability: Output layer updates correlate more directly with task performance, avoiding the entangled representations of deeper layers.

By leveraging the output layer’s sensitivity and computational tractability, our approach balances theoretical rigor with practical feasibility, enabling lightweight yet effective data pruning during SFT. Our experiments further validate this choice in § 4.3, showing that data selected based on output layer metrics generalizes effectively across architectures, with pruning decisions from smaller models transferring to larger ones.

Applying this, we obtained a simplified version of (1) and (2) as:

$$\text{DON} = \|W^L\|_F - \|W'^L\|_F = \sqrt{\sum_{i=1}^{m_L} \sum_{j=1}^{n_L} |w_{i,j}^L|^2} - \sqrt{\sum_{i=1}^{m_L} \sum_{j=1}^{n_L} |w'^L_{i,j}|^2}, \quad (3)$$

where m_L and n_L are the dimensions of the output layer.

$$\text{NOD} = \|W^L - W'^L\|_F = \sqrt{\sum_{i=1}^{m_L} \sum_{j=1}^{n_L} |w_{i,j}^L - w'^L_{i,j}|^2}. \quad (4)$$

3.3.2 Integration of TOPSIS

TOPSIS is a multi-criteria decision analysis (MCDA) method that ranks alternatives by their relative closeness to an ideal solution. In DONOD, TOPSIS is employed to resolve the inherent tension between the two metrics—DON and NOD—by identifying samples that simultaneously maximize DON (to enhance generalization) and minimize NOD (to avoid noisy or harmful updates). After computing the DON and NOD for each sample, we integrate TOPSIS to rank samples. Details of the algorithm can be found in Appendix A.5.

TOPSIS inherently balances conflicting objectives (maximizing DON and minimizing NOD) by leveraging geometric distance in the normalized metric space. Moreover, normalization mitigates the impact of differing metric magnitudes, ensuring neither DON nor NOD dominates the ranking. It avoids subjective weight assignment (unlike weighted sum) and provides a total ordering of samples (unlike Pareto optimality), which is critical for deterministic pruning decisions. These factors make TOPSIS considered as particularly suitable here.

4 Experiment

4.1 Experiment Setup

Evaluation Benchmarks and Training Datasets Following Ma et al. (2025), we constructed our evaluation benchmark based on AGIEval from Zhong et al. (2024) and IFEval from Zhou et al. (2023). This benchmark is designed to be comprehensive and domain-orthogonal, measuring abilities in logical reasoning, mathematics, reading comprehension, and instruction following. By incorporating diverse datasets, the benchmark closely mirrors real-world scenarios of ad-hoc SFT, where the goal is to enhance specific abilities of the model rather than simply improving performance on a limited and unrepresentative benchmark. The details of the benchmark are shown in Table A.1.

For training datasets, we experimented with DONOD on two different datasets to demonstrate its dataset-agnostic nature and applicability across domains, regardless of the availability of a validation

set. For mathematical problem-solving, we chose the SAT Math Chain-of-Thought (COT) dataset from Davidson (2023), which is constructed from the real-world Scholastic Assessment Test (SAT) question test-bank. This dataset provides no validation set, but its distribution closely aligns with the SAT-math test set. We show that DONOD generalizes well not only to closely related distributions but also to other math domains and unrelated tasks. Conversely, we also selected the LogiQA-Train dataset from Liu et al. (2020), which includes both a training set and a validation set. Unlike the SAT Math dataset, LogiQA is not COT labeled, providing only the correct option letter as the answer for each multiple-choice question. The details of the training datasets are shown in Table 5.

Models and Experiment Settings DONOD is evaluated on three models: Llama-3.2-3B-Instruct Meta AI (2024), Llama-3.1-8B-Instruct Grattafiori et al. (2024), and Llama-2-13b-chat Touvron et al. (2023). These models were chosen to demonstrate the generalization of DONOD across different architectures and fine-tuning paradigms: Llama-3.2-3B-Instruct is a smaller model optimized for instruction following, while Llama-2-13b-chat is a larger model fine-tuned for chat-based tasks. The results show that DONOD generalizes well across both cross-architecture and supervised fine-tuned models. As discussed in § 3.3.1, we select $l = 32$, the `lm_head` layer (i.e., the output layer) of the Llama-3.1-8B-Instruct model, for our experiments. Additional details on training configurations can be found in Appendix A.2. For ablations, we trained the Llama-3.1-8B-Instruct model with the SAT Math COT dataset pruned by the different configurations of alternative DONOD. The other training settings remain the same as the main settings.

4.2 Baselines

DONOD is compared with four baselines to evaluate its effectiveness. These baselines starts from random pruning, the full dataset. Additionally, to account for the model-intrinsic nature of DONOD, we compare it with two advanced methods that do not rely on external models: Instruction Following Difficulty (IFD) and Low-rank gradiEnt Similarity Search (LESS).

IFD, proposed by Li et al. (2024), selects data based on a novel metric, the Instruction Following Difficulty. This metric is measured by the ratio of losses for the same sample obtained with and without the instruction in the prompt. IFD assumes that samples where instructions significantly aid the model in producing the expected output should be prioritized. However, IFD has limitations. For datasets like LogiQA, where each sample is labeled with a single character, the oversimplified nature of the labels reduces IFD’s sensitivity and effectiveness. Furthermore, IFD relies on datasets in the Alpaca format, which requires a clear separation between instructions and input. For datasets like OpenAI’s, where the input consists of a single prompt, IFD is less efficient.

Regarding this, we also compare DONOD with LESS, a gradient-based method proposed by Xia et al. (2024). LESS selects influential data for instruction tuning by measuring gradient similarity between training examples and a target task. Unlike IFD, LESS has no specific dataset format requirements and does not overly rely on labels. However, LESS requires a clear target data distribution, meaning it necessitates a development set. This constraint limits its applicability in scenarios where such a set is unavailable.

Given the constraints of IFD and LESS, as well as the characteristics of the benchmarks (see Table 5), we train and evaluate IFD on the LogiQA-Train dataset and LESS on the SAT Math COT dataset. For a fair comparison, we follow the best settings reported in the respective papers and compare the results with the same amount or even less of data pruned by DONOD.

4.3 Main Results

Empirical Validation of Output Layer Focus To further justify our design choice in § 3.3.1, we analyze the sensitivity of weight changes across layers. Figure 3 ranks the Frobenius norm delta across layers after fine-tuning Llama-2-13B-Chat on the SAT Math COT dataset. The output layer (`lm_head`) shows the largest delta. We also tested on more models, details can be found in Appendix A.8. By restricting DON/NOD computations to this layer, we retain of the total Frobenius signal (averaged across layers) while reducing computational costs to negligible. Comparing with complete backpropagation and compute DON_{total} and NOD_{total} across all layers for every single data sample, this only require backpropagation of the last layer of the model together with a constant time DON and NOD computation.

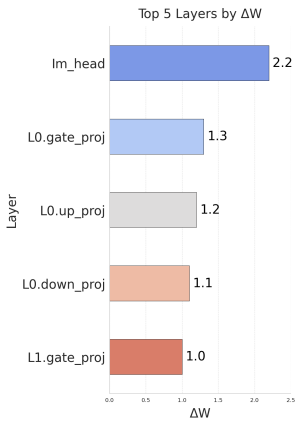


Figure 3: Rank of the top 5 layers by Frobenius norm delta after fine-tuning Llama-2-13B-Chat on SAT Math COT

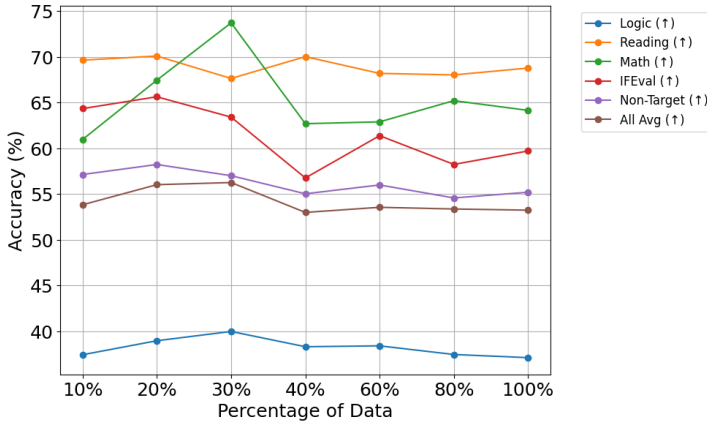


Figure 4: Stability of DONOD across data proportions. Performance peaks at 20%-30% of data (optimal balance for Logic, Reading, and Overall Average), with Math scores steadily improving up to 30%. Notably, 10% DONOD-selected data outperforms full-dataset training (100%) in Logic and Overall Average, demonstrating robustness and efficiency.

Stability of DONOD Across Data Proportions and Model Architecture To evaluate the stability of DONOD under varying data regimes, we analyze its performance when trained on subsets of the dataset (10%–100%). As shown in Figure 4, DONOD demonstrates remarkable stability and efficiency, achieving competitive or superior performance even with significantly reduced data.

Notably, with only 10% of the data, DONOD surpasses the full-dataset (100%) baseline in Logic (37.43 vs. 37.12) and Overall Average (53.82 vs. 53.23), highlighting its robustness against data scarcity. At 20% data, the method reaches an optimal balance between data efficiency and model performance, achieving peak scores in Logic (38.96) and Reading (70.08), while maintaining strong Overall Average (56.01). This suggests DONOD effectively identifies high-quality samples that maximize learning signals with minimal noise. Similar results are obtained on Llama-3.2-3B-Instruct and Llama-2-13b-chat, detailed results can be found in Appendix A.4.

A key finding is the steady improvement in mathematical reasoning as data increases to 30% (73.70), outperforming all other configurations. This aligns with DONOD’s ability to retain domain-critical samples that enhance specialized capabilities without overfitting. Beyond 30%, performance in most categories plateaus or declines slightly, indicating diminishing returns from additional data—a hallmark of DONOD’s precision in filtering redundant or harmful samples.

Table 1: Experimental results with domain-specific averages. The **Non-Target** column shows average performance excluding mathematical reasoning (target domain), revealing how methods generalize to other abilities. All values are percentages.

Configuration	Logic (↑)	Reading (↑)	Math (↑)	IFEval (↑)	Non-Target (↑)	All Avg (↑)
IFD 40%	39.31	68.26	64.18	63.03	56.87	55.04
Random 40%	38.32	69.72	61.17	59.89	55.98	53.15
ALL 100%	37.12	68.76	64.14	59.70	55.19	53.23
DONOD 20%	38.96	70.08	67.44	65.62	58.22	56.01

Comparison with Baselines As shown in Table 1 and 2, DONOD achieves superior overall performance across both experiments, despite using less data than baselines and requiring no development set. While minor trade-offs exist in some domains (e.g., logic at 5%: 20.91 vs. LESS’s 22.62), DONOD balances task-specific gains and cross-domain stability effectively.

Being more specific, with 20% data, DONOD surpasses IFD (40% data) by +0.97 All Avg (56.01 vs. 55.04) and outperforms the full dataset by +2.78. At 5% data, DONOD exceeds LESS (5%) by 0.95

Table 2: Experimental results comparing LESS with other methods at 5% data selection. The **Non-Target** column shows average performance excluding logic reasoning (target domain), revealing how methods generalize to other abilities. All values are percentages.

Method	Logic (↑)	Reading (↑)	Math (↑)	IFEval (↑)	Non-Target (↑)	All Avg (↑)
LESS 5%	22.62	25.19	21.47	64.33	36.99	27.91
Random 5%	20.45	24.27	24.06	46.95	31.96	26.35
ALL 100%	22.98	24.02	22.26	17.74	21.34	22.77
DONOD 5%	20.91	24.27	24.22	68.95	39.15	28.86

All Avg (28.86 vs. 27.91) and improves over 100% data by +6.09, showcasing robustness to extreme sparsity. Also, our method shows a well target-generalization balance, in the target domain (math), DONOD achieves SOTA (67.44 at 20%, 24.22 at 5%), proving its ability to prioritize task-critical samples. Despite slight logic/reading trade-offs (e.g., 20.91 vs. LESS’s 22.62), DONOD retains best-in-class cross-domain performance (Non-Target: 58.22 at 20%, 39.15 at 5%), outperforming all baselines. Considering DONOD requires no development set and works seamlessly across both CoT (SAT Math) and non-CoT (LogiQA) datasets, such a minor trade-off should be acceptable.

4.4 Ablation Experiments Results

As shown in Table 4, We evaluate four configurations: (1) DON-only ranking, (2) NOD-only ranking, (3) DON + NOD combinations without TOPSIS (Weighted Sum and Pareto Front), and (4) the full method (DON + NOD + TOPSIS). Notably, we omit ablations combining TOPSIS with only one metric (e.g., DON + TOPSIS or NOD + TOPSIS) because TOPSIS inherently requires multiple criteria to resolve conflicting rankings. Applying TOPSIS to a single metric reduces it to a trivial ranking equivalent to using the metric alone, offering no performance gain. Results are presented in Table 3, revealing distinct roles for each component in balancing domain-specific performance and cross-domain generalization.

Table 3: Experimental results with domain-specific averages. The **Non-Target** column shows average performance (%) excluding mathematical reasoning (target domain), revealing how methods generalize to other abilities.

Configuration	Logic (↑)	Reading (↑)	Math (↑)	IFEval (↑)	Non-Target (↑)	All Avg (↑)
DON	36.19	68.12	58.15	66.17	56.83	52.38
NOD	40.23	67.12	65.71	58.04	55.13	54.39
Weight Sum	38.08	69.15	63.74	53.79	53.67	53.54
Pareto Optimization	36.85	70.02	57.82	65.25	57.37	53.07
DONOD	38.96	70.08	67.44	65.62	58.22	56.01

Impact of Individual Metrics Using NOD alone improves target-domain performance (e.g., Math: 65.71% vs. DON’s 58.15%), as NOD prioritizes samples that can best boost model’s performance of the corresponding domain. However, this comes at the cost of reduced non-target generalization (55.13% vs. DON’s 56.83%), indicating over-specialization. Conversely, DON alone achieves better cross-domain robustness (Non-Target: 56.83%) by filtering samples with that harms the cross-domain generalization, though it lags in target-domain adaptation.

Combination Strategies Combining DON and NOD via naive strategies like Weighted Sum or Pareto Front fails to harmonize their strengths. Weighted Sum marginally improves Reading (69.15%) but degrades Math (63.74%) and Non-Target (53.67%) compared to single metrics. Pareto Front prioritizes stability (Non-Target: 57.37%) but sacrifices target-domain gains (Math: 57.82%). Both strategies highlight the challenge of balancing conflicting metrics without a principled integration method.

Full Method (DONOD) Integrating DON, NOD, and TOPSIS achieves optimal balance. TOPSIS resolves metric conflicts by ranking samples based on their proximity to ideal DON/NOD values,

improving target-domain accuracy (Math: 67.44%, +1.73% over NOD) while preserving cross-domain robustness (Non-Target: 58.22%, +1.39% over DON). The full method also dominates in overall performance (All Avg: 56.01%, +2.47% over Weight Sum), validating the necessity of TOPSIS for multi-objective optimization.

4.5 More Analytical Results

Computational Complexity The algorithm’s computational complexity consists of two phases: (1) per-sample DON and NOD computation and (2) TOPSIS-based sample selection.

In the first phase, we perform a forward pass ($O(P)$ time per sample, where P is the model’s parameter count), a backward pass restricted to the output layer ($O(O)$ time, O being the output layer’s parameters), and compute Frobenius norms for weight updates ($O(O)$). Since $O \subset P$, the per-sample cost simplifies to $O(P)$, resulting in a total training complexity of $O(N \cdot P)$, where N is the number of training samples.

The second phase involves normalizing DON/NOD metrics ($O(N)$), computing distances to ideal and negative-ideal solutions ($O(N)$), and ranking samples via TOPSIS scores, dominated by an $O(N \log N)$ sorting step. Thus, the selection process has a total complexity of $O(N \log N)$.

Combining both phases, the dominant term is $O(N \cdot P)$, as $P \gg N \log N$ in modern neural networks (e.g., $P \sim 10^6-10^{12}$ parameters). The overall time complexity simplifies to $O(N \cdot P)$. For storage, only $O(N)$ space is required to store per-sample metrics, as no intermediate model states need to be retained. Therefore, the runtime of DONOD can be approximated by the model’s inference speed. In our experiments using Llama-3.1-8B-Instruct, processing the SAT Math COT dataset took approximately 18 minutes of wall-clock time on a single A100 80GB GPU, with negligible storage requirements.

Human Evaluation on Pruned Dataset To rigorously demonstrate the effectiveness of DONOD, a human evaluation was conducted. By reversing the selection process, where the top N samples with the highest TOPSIS scores are retained, NODON generates a dataset containing the top samples that DONOD would filter out. As illustrated in Figure 5, these samples tend to cluster on the right side of the NOD-DON plane.

To further analyze the data pruned by our method, we examined samples from the NODON-pruned SAT Math COT datasets. The evaluation revealed several common categories of pruned samples: 1) Overthinking in response to easy questions, 2) Incomplete or partial answers, 3) Incorrect answers due to reasoning errors, 4) Incorrect answers resulting from errors in the question itself, 5) Overly complex or excessively difficult questions.

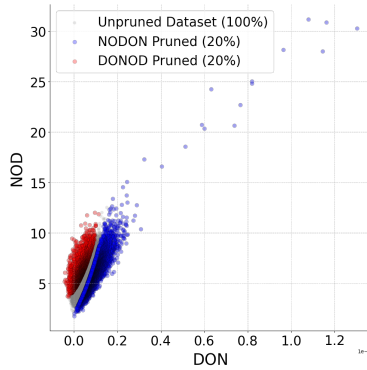


Figure 5: Illustration of the distribution of pruned dataset with DONOD and NODON (keep samples with the lowest TOPSIS scores, efficiently samples with high NOD and low DON).

5 Conclusion

In this paper, we propose DONOD, a model-intrinsic dataset pruning framework for LLM SFT. Based on the model’s weight dynamics, our framework leverages dual complementary metrics, DON and NOD. DON captures the cumulative shifts in model weight magnitudes while NOD quantifies the instability caused by individual samples. Thus, DON prioritizes samples with stable cross-domain generalization, and NOD filters out noisy or unlearnable samples. Integrated by TOPSIS, our dataset pruning framework effectively balances the objective of maximizing generalization and minimizing harmful updates. Extensive experiment results demonstrate that our framework can significantly reduce training data volume (e.g., reducing 70%) with performance improvement compared to

standard SFT. Meanwhile, the pruned datasets exhibit superior cross-architecture generalization. Datasets pruned by smaller models can generalize well on larger architectures, further enhancing the practicality.

References

- Peter Bartlett. For valid generalization the size of the weights is more important than the size of the network. In M.C. Mozer, M. Jordan, and T. Petsche (eds.), *Advances in Neural Information Processing Systems*, volume 9. MIT Press, 1996. URL https://proceedings.neurips.cc/paper_files/paper/1996/file/fb2fcd534b0ff3bbbed73cc51df620323-Paper.pdf.
- Yihan Cao, Yanbin Kang, Chi Wang, and Lichao Sun. Instruction mining: Instruction data selection for tuning large language models, 2024. URL <https://arxiv.org/abs/2307.06290>.
- Hao Chen, Yiming Zhang, Qi Zhang, Hantao Yang, Xiaomeng Hu, Xuetao Ma, Yifan Yanggong, and Junbo Zhao. Maybe only 0.5 URL <https://arxiv.org/abs/2305.09246>.
- Lichang Chen, Shiyang Li, Jun Yan, Hai Wang, Kalpa Gunaratna, Vikas Yadav, Zheng Tang, Vijay Srinivasan, Tianyi Zhou, Heng Huang, and Hongxia Jin. Alpapasus: Training a better alpaca with fewer data, 2024. URL <https://arxiv.org/abs/2307.08701>.
- Nathan Davidson. Sat math chain-of-thought dataset, 2023. URL <https://huggingface.co/datasets/ndavidson/sat-math-chain-of-thought>. Accessed: 2024-10-26.
- Qianlong Du, Chengqing Zong, and Jiajun Zhang. Mods: Model-oriented data selection for instruction tuning, 2023. URL <https://arxiv.org/abs/2311.15653>.
- Aaron Grattafiori, Abhimanyu Dubey, Abhinav Jauhri, Abhinav Pandey, Abhishek Kadian, Ahmad Al-Dahle, Aiesha Letman, Akhil Mathur, Alan Schelten, Alex Vaughan, Amy Yang, Angela Fan, Anirudh Goyal, Anthony Hartshorn, Aobo Yang, Archi Mitra, Archie Sravankumar, Artem Korenev, Arthur Hinsvark, Arun Rao, Aston Zhang, Aurelien Rodriguez, Austen Gregerson, Ava Spataru, Baptiste Roziere, Bethany Biron, Binh Tang, Bobbie Chern, Charlotte Caucheteux, Chaya Nayak, Chloe Bi, Chris Marra, Chris McConnell, Christian Keller, Christophe Touret, Chunyang Wu, Corinne Wong, Cristian Canton Ferrer, Cyrus Nikolaidis, Damien Allonsius, Daniel Song, Danielle Pintz, Danny Livshits, Danny Wyatt, David Esiobu, Dhruv Choudhary, Dhruv Mahajan, Diego Garcia-Olano, Diego Perino, Dieuwke Hupkes, Egor Lakomkin, Ehab AlBadawy, Elina Lobanova, Emily Dinan, Eric Michael Smith, Filip Radenovic, Francisco Guzmán, Frank Zhang, Gabriel Synnaeve, Gabrielle Lee, Georgia Lewis Anderson, Govind Thattai, Graeme Nail, Gregoire Mialon, Guan Pang, Guillem Cucurell, Hailey Nguyen, Hannah Korevaar, Hu Xu, Hugo Touvron, Iliyan Zarov, Imanol Arrieta Ibarra, Isabel Kloumann, Ishan Misra, Ivan Evtimov, Jack Zhang, Jade Copet, Jaewon Lee, Jan Geffert, Jana Vranes, Jason Park, Jay Mahadeokar, Jeet Shah, Jelmer van der Linde, Jennifer Billock, Jenny Hong, Jenya Lee, Jeremy Fu, Jianfeng Chi, Jianyu Huang, Jiawen Liu, Jie Wang, Jiecao Yu, Joanna Bitton, Joe Spisak, Jongsoo Park, Joseph Rocca, Joshua Johnstun, Joshua Saxe, Junteng Jia, Kalyan Vasuden Alwala, Karthik Prasad, Kartikeya Upasani, Kate Plawiak, Ke Li, Kenneth Heafield, Kevin Stone, Khalid El-Arini, Krithika Iyer, Kshitiz Malik, Kuenley Chiu, Kunal Bhalla, Kushal Lakhotia, Lauren Rantala-Yearly, Laurens van der Maaten, Lawrence Chen, Liang Tan, Liz Jenkins, Louis Martin, Lovish Madaan, Lubo Malo, Lukas Blecher, Lukas Landzaat, Luke de Oliveira, Madeline Muzzi, Mahesh Pasupuleti, Mannat Singh, Manohar Paluri, Marcin Kardas, Maria Tsimpoukelli, Mathew Oldham, Mathieu Rita, Maya Pavlova, Melanie Kambadur, Mike Lewis, Min Si, Mitesh Kumar Singh, Mona Hassan, Naman Goyal, Narjes Torabi, Nikolay Bashlykov, Nikolay Bogoychev, Niladri Chatterji, Ning Zhang, Olivier Duchenne, Onur Çelebi, Patrick Alrassy, Pengchuan Zhang, Pengwei Li, Petar Vasic, Peter Weng, Prajjwal Bhargava, Pratik Dubal, Praveen Krishnan, Punit Singh Koura, Puxin Xu, Qing He, Qingxiao Dong, Ragavan Srinivasan, Raj Ganapathy, Ramon Calderer, Ricardo Silveira Cabral, Robert Stojnic, Roberta Raileanu, Rohan Maheswari, Rohit Girdhar, Rohit Patel, Romain Sauvestre, Ronnie Polidoro, Roshan Sumbaly, Ross Taylor, Ruan Silva, Rui Hou, Rui Wang, Saghar Hosseini, Sahana Chennabasappa, Sanjay Singh, Sean Bell, Seohyun Sonia Kim, Sergey Edunov, Shaoliang Nie, Sharan Narang, Sharath Rapparthi, Sheng Shen, Shengye Wan, Shruti Bhosale, Shun Zhang, Simon Vandenhende, Soumya Batra, Spencer Whitman, Sten Sootla, Stephane Collot, Suchin Gururangan,

Sydney Borodinsky, Tamar Herman, Tara Fowler, Tarek Sheasha, Thomas Georgiou, Thomas Scialom, Tobias Speckbacher, Todor Mihaylov, Tong Xiao, Ujjwal Karn, Vedanuj Goswami, Vibhor Gupta, Vignesh Ramanathan, Viktor Kerkez, Vincent Gonguet, Virginie Do, Vish Vogeti, Vitor Albiero, Vladan Petrovic, Weiwei Chu, Wenhan Xiong, Wenyin Fu, Whitney Meers, Xavier Martinet, Xiaodong Wang, Xiaofang Wang, Xiaoqing Ellen Tan, Xide Xia, Xinfeng Xie, Xuchao Jia, Xuewei Wang, Yaelle Goldschlag, Yashesh Gaur, Yasmine Babaei, Yi Wen, Yiwen Song, Yuchen Zhang, Yue Li, Yuning Mao, Zacharie Delpierre Coudert, Zheng Yan, Zhengxing Chen, Zoe Papanikos, Aaditya Singh, Aayushi Srivastava, Abha Jain, Adam Kelsey, Adam Shajnfeld, Adithya Gangidi, Adolfo Victoria, Ahuva Goldstand, Ajay Menon, Ajay Sharma, Alex Boesenberg, Alexei Baevski, Allie Feinstein, Amanda Kallet, Amit Sangani, Amos Teo, Anam Yunus, Andrei Lupu, Andres Alvarado, Andrew Caples, Andrew Gu, Andrew Ho, Andrew Poulton, Andrew Ryan, Ankit Ramchandani, Annie Dong, Annie Franco, Anuj Goyal, Aparajita Saraf, Arkabandhu Chowdhury, Ashley Gabriel, Ashwin Bharambe, Assaf Eisenman, Azadeh Yazdan, Beau James, Ben Maurer, Benjamin Leonhardi, Bernie Huang, Beth Loyd, Beto De Paola, Bhargavi Paranjape, Bing Liu, Bo Wu, Boyu Ni, Braden Hancock, Bram Wasti, Brandon Spence, Brani Stojkovic, Brian Gamido, Britt Montalvo, Carl Parker, Carly Burton, Catalina Mejia, Ce Liu, Changhan Wang, Changkyu Kim, Chao Zhou, Chester Hu, Ching-Hsiang Chu, Chris Cai, Chris Tindal, Christoph Feichtenhofer, Cynthia Gao, Damon Civin, Dana Beaty, Daniel Kreymmer, Daniel Li, David Adkins, David Xu, Davide Testuggine, Delia David, Devi Parikh, Diana Liskovich, Didem Foss, Dingkang Wang, Duc Le, Dustin Holland, Edward Dowling, Eissa Jamil, Elaine Montgomery, Eleonora Presani, Emily Hahn, Emily Wood, Eric-Tuan Le, Erik Brinkman, Esteban Arcaute, Evan Dunbar, Evan Smothers, Fei Sun, Felix Kreuk, Feng Tian, Filippos Kokkinos, Firat Ozgenel, Francesco Caggioni, Frank Kanayet, Frank Seide, Gabriela Medina Florez, Gabriella Schwarz, Gada Badeer, Georgia Swee, Gil Halpern, Grant Herman, Grigory Sizov, Guangyi, Zhang, Guna Lakshminarayanan, Hakan Inan, Hamid Shojanazeri, Han Zou, Hannah Wang, Hanwen Zha, Haroun Habeeb, Harrison Rudolph, Helen Suk, Henry Aspegren, Hunter Goldman, Hongyuan Zhan, Ibrahim Damlaj, Igor Molybog, Igor Tufanov, Ilias Leontiadis, Irina-Elena Veliche, Itai Gat, Jake Weissman, James Geboski, James Kohli, Janice Lam, Japhet Asher, Jean-Baptiste Gaya, Jeff Marcus, Jeff Tang, Jennifer Chan, Jenny Zhen, Jeremy Reizenstein, Jeremy Teboul, Jessica Zhong, Jian Jin, Jingyi Yang, Joe Cummings, Jon Carvill, Jon Shepard, Jonathan McPhee, Jonathan Torres, Josh Ginsburg, Junjie Wang, Kai Wu, Karan Hou U, Karan Saxena, Kartikay Khandelwal, Katayoun Zand, Kathy Matosich, Kaushik Veeraraghavan, Kelly Michelena, Keqian Li, Kiran Jagadeesh, Kun Huang, Kunal Chawla, Kyle Huang, Lailin Chen, Lakshya Garg, Lavender A, Leandro Silva, Lee Bell, Lei Zhang, Liangpeng Guo, Licheng Yu, Liron Moshkovich, Luca Wehrstedt, Madian Khabza, Manav Avalani, Manish Bhatt, Martynas Mankus, Matan Hasson, Matthew Lennie, Matthias Reso, Maxim Groshev, Maxim Naumov, Maya Lathi, Meghan Keneally, Miao Liu, Michael L. Seltzer, Michal Valko, Michelle Restrepo, Mihir Patel, Mik Vyatskov, Mikayel Samvelyan, Mike Clark, Mike Macey, Mike Wang, Miquel Jubert Hermoso, Mo Metanat, Mohammad Rastegari, Munish Bansal, Nandhini Santhanam, Natascha Parks, Natasha White, Navyata Bawa, Nayan Singhal, Nick Egebo, Nicolas Usunier, Nikhil Mehta, Nikolay Pavlovich Laptev, Ning Dong, Norman Cheng, Oleg Chernoguz, Olivia Hart, Omkar Salpekar, Ozlem Kalinli, Parkin Kent, Parth Parekh, Paul Saab, Pavan Balaji, Pedro Rittner, Philip Bontrager, Pierre Roux, Piotr Dollar, Polina Zvyagina, Prashant Ratanchandani, Pritish Yuvraj, Qian Liang, Rachad Alao, Rachel Rodriguez, Rafi Ayub, Raghotham Murthy, Raghu Nayani, Rahul Mitra, Rangaprabhu Parthasarathy, Raymond Li, Rebekkah Hogan, Robin Battey, Rocky Wang, Russ Howes, Ruty Rinott, Sachin Mehta, Sachin Siby, Sai Jayesh Bondu, Samyak Datta, Sara Chugh, Sara Hunt, Sargun Dhillon, Sasha Sidorov, Satadru Pan, Saurabh Mahajan, Saurabh Verma, Seiji Yamamoto, Sharadh Ramaswamy, Shaun Lindsay, Sheng Feng, Shenghao Lin, Shengxin Cindy Zha, Shishir Patil, Shiva Shankar, Shuqiang Zhang, Shuqiang Zhang, Sinong Wang, Sneha Agarwal, Soji Sajuyigbe, Soumith Chintala, Stephanie Max, Stephen Chen, Steve Kehoe, Steve Satterfield, Sudarshan Govindaprasad, Sumit Gupta, Summer Deng, Sungmin Cho, Sunny Virk, Suraj Subramanian, Sy Choudhury, Sydney Goldman, Tal Remez, Tamar Glaser, Tamara Best, Thilo Koehler, Thomas Robinson, Tianhe Li, Tianjun Zhang, Tim Matthews, Timothy Chou, Tzook Shaked, Varun Vontimitta, Victoria Ajayi, Victoria Montanez, Vijai Mohan, Vinay Satish Kumar, Vishal Mangla, Vlad Ionescu, Vlad Poenaru, Vlad Tiberiu Mihailescu, Vladimir Ivanov, Wei Li, Wenchen Wang, Wenwen Jiang, Wes Bouaziz, Will Constable, Xiaocheng Tang, Xiaojian Wu, Xiaolan Wang, Xilun Wu, Xinbo Gao, Yaniv Kleinman, Yanjun Chen, Ye Hu, Ye Jia, Ye Qi, Yenda Li, Yilin Zhang, Ying Zhang, Yossi Adi, Youngjin Nam, Yu, Wang, Yu Zhao, Yuchen Hao, Yundi Qian, Yunlu Li, Yuzi He, Zach Rait, Zachary DeVito, Zef Rosnbrick, Zhaoduo Wen, Zhenyu Yang, Zhiwei Zhao, and Zhiyu Ma. The

- llama 3 herd of models, 2024. URL <https://arxiv.org/abs/2407.21783>.
- Angela H. Jiang, Daniel L. K. Wong, Giulio Zhou, David G. Andersen, Jeffrey Dean, Gregory R. Ganger, Gauri Joshi, Michael Kaminsky, Michael Kozuch, Zachary C. Lipton, and Padmanabhan Pillai. Accelerating deep learning by focusing on the biggest losers, 2019. URL <https://arxiv.org/abs/1910.00762>.
- Dawei Li, Renliang Sun, Yue Huang, Ming Zhong, Bohan Jiang, Jiawei Han, Xiangliang Zhang, Wei Wang, and Huan Liu. Preference leakage: A contamination problem in llm-as-a-judge, 2025. URL <https://arxiv.org/abs/2502.01534>.
- Ming Li, Yong Zhang, Zhitao Li, Jiuhai Chen, Lichang Chen, Ning Cheng, Jianzong Wang, Tianyi Zhou, and Jing Xiao. From quantity to quality: Boosting llm performance with self-guided data selection for instruction tuning, 2024. URL <https://arxiv.org/abs/2308.12032>.
- Jian Liu, Leyang Cui, Hanmeng Liu, Dandan Huang, Yile Wang, and Yue Zhang. Logiqa: A challenge dataset for machine reading comprehension with logical reasoning, 2020. URL <https://arxiv.org/abs/2007.08124>.
- Wei Liu, Weihao Zeng, Keqing He, Yong Jiang, and Junxian He. What makes good data for alignment? a comprehensive study of automatic data selection in instruction tuning, 2024. URL <https://arxiv.org/abs/2312.15685>.
- Ilya Loshchilov and Frank Hutter. Online batch selection for faster training of neural networks, 2016. URL <https://arxiv.org/abs/1511.06343>.
- Ilya Loshchilov and Frank Hutter. Decoupled weight decay regularization, 2019. URL <https://arxiv.org/abs/1711.05101>.
- Kaijing Ma, Xeron Du, Yunran Wang, Haoran Zhang, ZhoufutuWen, Xingwei Qu, Jian Yang, Jiaheng Liu, minghao liu, Xiang Yue, Wenhao Huang, and Ge Zhang. KOR-bench: Benchmarking language models on knowledge-orthogonal reasoning tasks. In *The Thirteenth International Conference on Learning Representations*, 2025. URL <https://openreview.net/forum?id=SVRRQ8goQo>.
- Meta AI. Llama 3.2: Revolutionizing edge AI and vision with open, customizable models. Retrieved from <https://ai.meta.com/blog/llama-3-2-connect-2024-vision-edge-mobile-devices/>, September 2024. Accessed: March 27, 2025.
- Sören Mindermann, Jan Brauner, Muhammed Razzak, Mrinank Sharma, Andreas Kirsch, Winnie Xu, Benedikt Höltingen, Aidan N. Gomez, Adrien Morisot, Sebastian Farquhar, and Yarin Gal. Prioritized training on points that are learnable, worth learning, and not yet learnt, 2022. URL <https://arxiv.org/abs/2206.07137>.
- Suneel Nadipalli. Layer-wise evolution of representations in fine-tuned transformers: Insights from sparse autoencoders, 2025. URL <https://arxiv.org/abs/2502.16722>.
- Domenic Rosati, Jan Wehner, Kai Williams, Lukasz Bartoszcze, Robie Gonzales, carsten maple, Subhabrata Majumdar, Hassan Sajjad, and Frank Rudzicz. Representation noising: A defence mechanism against harmful finetuning. In *The Thirty-eighth Annual Conference on Neural Information Processing Systems*, 2024. URL <https://openreview.net/forum?id=eP9auEJqFg>.
- Shai Shalev-Shwartz and Shai Ben-David. *Understanding Machine Learning: From Theory to Algorithms*. Cambridge University Press, USA, 2014. ISBN 1107057132.
- Hugo Touvron, Louis Martin, Kevin Stone, Peter Albert, Amjad Almahairi, Yasmine Babaei, Nikolay Bashlykov, Soumya Batra, Prajjwal Bhargava, Shrutu Bhosale, Dan Bikel, Lukas Blecher, Cristian Canton Ferrer, Moya Chen, Guillem Cucurull, David Esiobu, Jude Fernandes, Jeremy Fu, Wenyin Fu, Brian Fuller, Cynthia Gao, Vedanuj Goswami, Naman Goyal, Anthony Hartshorn, Saghar Hosseini, Rui Hou, Hakan Inan, Marcin Kardas, Viktor Kerkez, Madian Khabsa, Isabel Kloumann, Artem Korenev, Punit Singh Koura, Marie-Anne Lachaux, Thibaut Lavril, Jenya Lee,

Diana Liskovich, Yinghai Lu, Yuning Mao, Xavier Martinet, Todor Mihaylov, Pushkar Mishra, Igor Molybog, Yixin Nie, Andrew Poulton, Jeremy Reizenstein, Rashi Rungta, Kalyan Saladi, Alan Schelten, Ruan Silva, Eric Michael Smith, Ranjan Subramanian, Xiaoqing Ellen Tan, Binh Tang, Ross Taylor, Adina Williams, Jian Xiang Kuan, Puxin Xu, Zheng Yan, Iliyan Zarov, Yuchen Zhang, Angela Fan, Melanie Kambadur, Sharan Narang, Aurelien Rodriguez, Robert Stojnic, Sergey Edunov, and Thomas Scialom. Llama 2: Open foundation and fine-tuned chat models, 2023. URL <https://arxiv.org/abs/2307.09288>.

Jiachen T. Wang, Tong Wu, Dawn Song, Prateek Mittal, and Ruoxi Jia. GREATS: Online selection of high-quality data for LLM training in every iteration. In *The Thirty-eighth Annual Conference on Neural Information Processing Systems*, 2024. URL <https://openreview.net/forum?id=232VcN8tSx>.

Mengzhou Xia, Sadhika Malladi, Suchin Gururangan, Sanjeev Arora, and Danqi Chen. Less: Selecting influential data for targeted instruction tuning, 2024. URL <https://arxiv.org/abs/2402.04333>.

Dong Yin, Kannan Ramchandran, and Peter Bartlett. Rademacher complexity for adversarially robust generalization, 2020. URL <https://arxiv.org/abs/1810.11914>.

Wanjun Zhong, Ruixiang Cui, Yiduo Guo, Yaobo Liang, Shuai Lu, Yanlin Wang, Amin Saied, Weizhu Chen, and Nan Duan. AGIEval: A human-centric benchmark for evaluating foundation models. In Kevin Duh, Helena Gomez, and Steven Bethard (eds.), *Findings of the Association for Computational Linguistics: NAACL 2024*, pp. 2299–2314, Mexico City, Mexico, June 2024. Association for Computational Linguistics. doi: 10.18653/v1/2024.findings-naacl.149. URL <https://aclanthology.org/2024.findings-naacl.149/>.

Jeffrey Zhou, Tianjian Lu, Swaroop Mishra, Siddhartha Brahma, Sujoy Basu, Yi Luan, Denny Zhou, and Le Hou. Instruction-following evaluation for large language models, 2023. URL <https://arxiv.org/abs/2311.07911>.

A Appendix

A.1 Benchmark Details

Table 4: Constructed Benchmark Details. To ensure the representativity of each measured ability, multiple datasets focusing on the same ability are selected, mitigating potential biases arising from the limited scope of individual exams. Additionally, the inclusion of the comprehensive and unrelated dataset IFEval-en further enhances the reliability and representative of the benchmark, aligning it more closely with real-world use cases.

Dataset	Ability	Validation Set Available	Test Set Size
LSAT-AR	Logical Reasoning	False	230
LSAT-LR	Logical Reasoning	False	510
LogiQA-en	Logical Reasoning	True	651
LSAT-RC	Reading Comprehension	False	269
SAT-en	Reading Comprehension	False	206
AQUA-RAT	Mathematical Problem-Solving	True	254
SAT-math	Mathematical Problem-Solving	False	220
IFEval-en	Instruction Following	False	541

A.2 Training Settings

- Global batch size: 16
- Micro-batch size: 1
- Learning rate: 2e-5
- Optimizer: AdamW (Loshchilov & Hutter (2019))
- Warmup-ratio 0.025
- Every model is trained on 8 NVIDIA A100 GPUs for less than 1 hour

A.3 Datasets Details

Table 5: Details of the datasets used in the study.

Dataset	Ability	Label Type	Size
LogiQA Train	Logic Reasoning	Single letter only	7,851
SAT Math COT	Mathematical Problem-Solving	COT	32,444

A.4 Cross Architecture Results

Table 6: Experimental results comparing different methods on Llama-2-13b-chat. The **Non-Target** column shows average performance excluding mathematical reasoning (target domain), revealing how methods generalize to other abilities. All values are percentages.

Method	Logic (↑)	Reading (↑)	Math (↑)	IFEval (↑)	Non-Target (↑)	All Avg (↑)
ALL (100%)	30.57	54.68	23.38	29.94	38.39	35.28
DONOD 20%	31.52	55.58	26.89	29.39	38.83	36.57
DONOD 30%	31.30	54.61	23.39	29.57	38.49	35.53

Table 7: Experimental results comparing different methods on Llama-3.2-3B-Instruct. The **Non-Target** column shows average performance excluding mathematical reasoning (target domain), revealing how methods generalize to other abilities. All values are percentages.

Method	Logic (↑)	Reading (↑)	Math (↑)	IFEval (↑)	Non-Target (↑)	All Avg (↑)
ALL (100%)	9.23	34.67	10.60	63.96	35.95	23.10
DONOD 20%	27.65	50.46	34.78	65.80	47.97	38.71
DONOD 30%	29.46	56.75	33.92	65.06	50.42	41.03

A.5 Integration with TOPSIS

1. Normalization: DON and NOD are normalized to eliminate scale differences. Given a matrix $W \in \mathbb{R}^{n \times 2}$, where n is the number of samples and columns represent DON and NOD, vector normalization is applied:

$$\tilde{w}_{i,j} = \frac{w_{i,j}}{\sqrt{\sum_{k=1}^n w_{k,j}^2}}. \quad (5)$$

2. Ideal Solutions: The hypothetical ideal solution Z^+ and negative-ideal solution Z^- are defined as:

$$Z^+ = [\max(\tilde{W}_{\text{DON}}), \min(\tilde{W}_{\text{NOD}})], \quad Z^- = [\min(\tilde{W}_{\text{DON}}), \max(\tilde{W}_{\text{NOD}})]. \quad (6)$$

These represent the hypothetical "best" and "worst" cases, where DON is maximized and NOD minimized (for Z^+), and vice versa (for Z^-).

3. Distance Calculation: The Euclidean distance of each sample to Z^+ and Z^- is computed:

$$D_i^+ = \sqrt{\sum_{j=1}^2 (\tilde{w}_{i,j} - Z_j^+)^2}, \quad D_i^- = \sqrt{\sum_{j=1}^2 (\tilde{w}_{i,j} - Z_j^-)^2}. \quad (7)$$

4. TOPSIS Score: The final score for each sample is:

$$C_i = \frac{D_i^-}{D_i^+ + D_i^-}, \quad (8)$$

where $C_i \in [0, 1]$. Higher scores indicate closer alignment with Z^+ and greater divergence from Z^- .

A.6 Ablation Configurations

Table 8: Ablation study configurations.

Configuration	DON	NOD	TOPSIS
DON Only	✓	×	×
NOD Only	×	✓	×
DON + NOD (Weighted Sum)	✓	✓	×
DON + NOD (Pareto Front)	✓	✓	×
DON + NOD + TOPSIS (Full)	✓	✓	✓

A.7 Bad Samples Gallery

How many edges does a cube have?

I need to identify how many edges a cube has. I remember that a cube is a three-dimensional shape with six square faces. Each square face has four edges, but when considering edges that are shared between two faces, I can't count all edges separately. A cube has 12 unique edges. They can be grouped into three sets of four edges that run parallel to each of the cube's three dimensions. Thus, after considering all faces and avoiding double counting, I confirm that the total number of edges in a cube is 12. \n Therefore the final answer is A cube has 12 edges.

Find the number of vertices of the rectangular prism.

I need to find the number of vertices of a rectangular prism. I know that a rectangular prism is a 3D shape with rectangular faces, length, width, and height. I can imagine that each corner of the prism is a vertex, and there are 2 corners at each edge. I can count 4 vertices at the top face, 4 vertices at the bottom face, and no additional vertices at the edges, since each edge has 2 vertices already counted. I conclude that there are $4 + 4 = 8$ vertices in a rectangular prism. \n Therefore the final answer is A rectangular prism has 8 vertices.

If you select three of the four numbers 1, 2, 3, and 4, allowing duplicates, and arrange them in a row to form a three-digit natural number. How many multiples of 3 are there? \n Therefore the final answer is There are 22 multiples of 3 that can be formed by selecting three of the four numbers 1, 2, 3, and 4 (allowing duplicates) and arranging them in a row to form a three-digit number.

What is the smallest number among the three numbers 5, 8, and 4?

I am asked to find the smallest number among three given numbers: 5, 8, and 4. I will compare the three numbers by looking at their values. I can see that 4 is the smallest number among the three, as it has the lowest value. \n Therefore the final answer is The smallest number among 5, 8, and 4 is 4.

The function $f(x)$ is defined as follows: $f(x) = 4 + \frac{\sqrt{x}}{16}$. \n What is the value of $f(144)$? \n A. 0 \n B. 16 \n C. 40 \n D. 76

We start by substituting 144 into the function $f(x)$. The function is defined as: $f(x) = 4 + \sqrt{x}$. So we need to calculate $f(144)$. Substituting 144 into the function, we have: $f(144) = 4 + \sqrt{144}$. Next, we calculate $\sqrt{144}$. The square root of 144 is 12. Now we can substitute this back into the function: $f(144) = 4 + 12$. Adding these values together gives: $f(144) = 16$. \n Therefore the final answer is 16

You subtracted 4.3 when you should have added 4.3 to a number, resulting in 8.8. Find the correct value.

\n Therefore the final answer is The correct value is 17.4.

Karen bakes 50 chocolate chip cookies. She keeps 10 for herself, and she gives 8 to her grandparents. Karen wants to give everyone in her class cookies. Each person in her class will receive 2 cookies. How many people are in Karen's class?

Therefore the final answer is Karen has 16 people in her class.

Ronnie is a train engineer. His train pulls 3 red boxcars, 4 blue boxcars, and 7 black boxcars. The black boxcars can each hold 4000 pounds of coal, and the red boxcars can hold 3 times as much as the blue boxcars. All of the train's boxcars combined can hold 132,000 pounds of coal. What is the ratio of the coal capacity of each black boxcar to each blue boxcar?

I understand that Ronnie's train has 3 red boxcars, 4 blue boxcars, and 7 black boxcars, and we need to find the ratio of the coal capacity of each black boxcar to each blue boxcar. I recognize that the black boxcars can hold 4000 pounds of coal, and the red boxcars can hold 3 times as much as the blue boxcars, and the total capacity of all boxcars is 132,000 pounds. I will let the coal capacity of each blue boxcar be B pounds, so each red boxcar can hold $3B$ pounds. I can write an equation based on the total capacity of all boxcars: $3(3B) + 4B + 7(4000) = 132,000$. I simplify the equation by combining like terms: $9B + 4B + 28,000 = 132,000$. I combine like terms to get: $13B + 28,000 = 132,000$. I subtract 28,000 from both sides to get: $13B = 104,000$, and then divide both sides by 13 to get: $B = 8,000$. I know that each blue boxcar can hold 8,000 pounds, and each black boxcar can hold 4,000 pounds, so the ratio of the coal capacity of each black boxcar to each blue boxcar is $4000/8000 = 1/2$.

\n Therefore the final answer is The ratio is 1:2.

A.8 Empirical Validations of Output Layer Focus

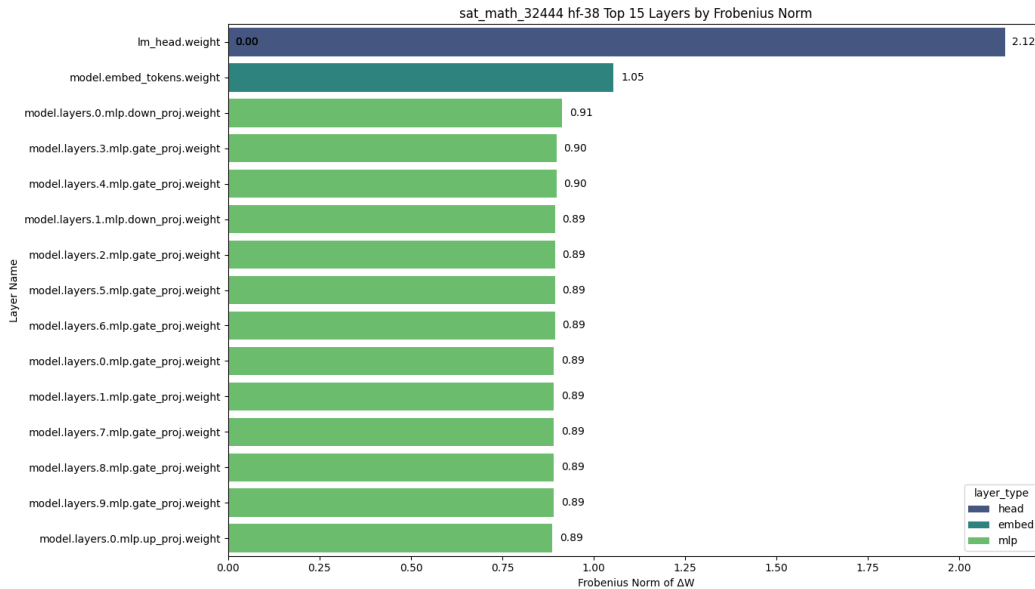


Figure 6: Ranking of Frobenius norm delta of layers of Llama-3.1-8B-Instruct after fine-tuning on SAT Math COT dataset, epoch 2

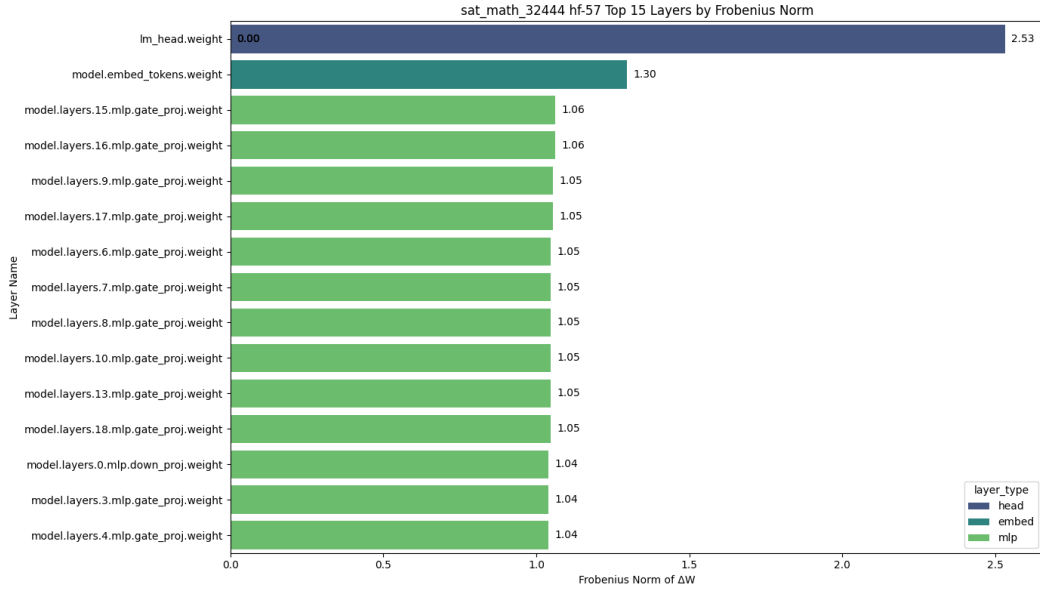


Figure 7: Ranking of Frobenius norm delta of layers of Llama-3.1-8B-Instruct after fine-tuning on SAT Math COT dataset, epoch 3

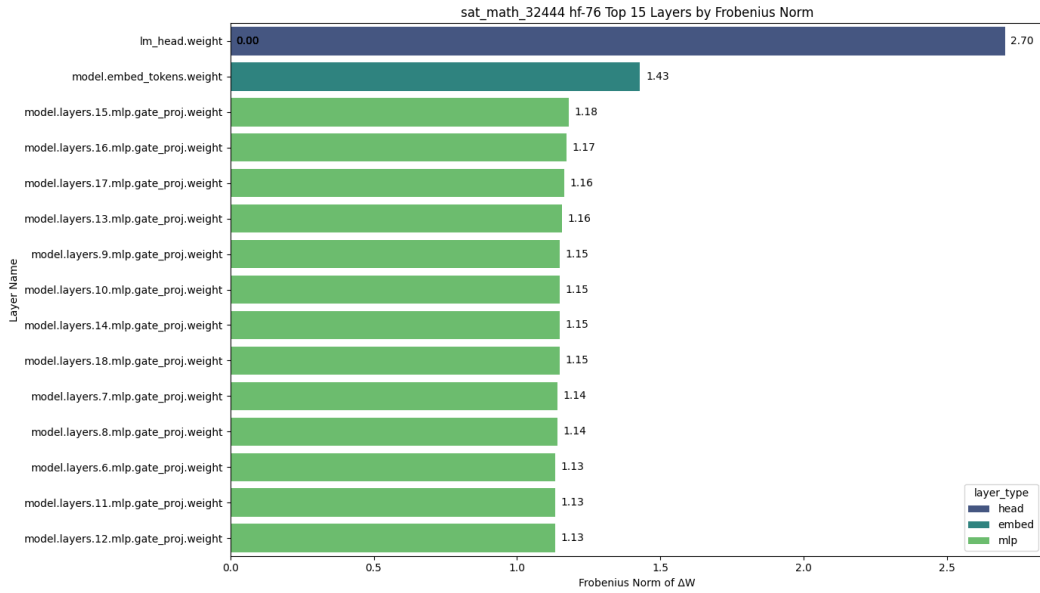


Figure 8: Ranking of Frobenius norm delta of layers of Llama-3.1-8B-Instruct after fine-tuning on SAT Math COT dataset, epoch 4

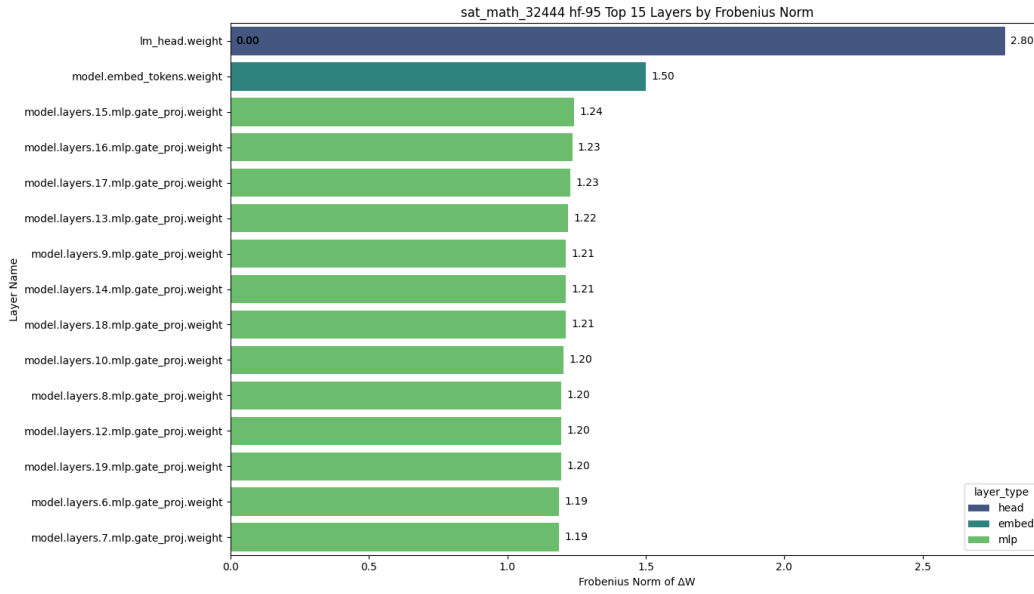


Figure 9: Ranking of Frobenius norm delta of layers of Llama-3.1-8B-Instruct after fine-tuning on SAT Math COT dataset, epoch 5

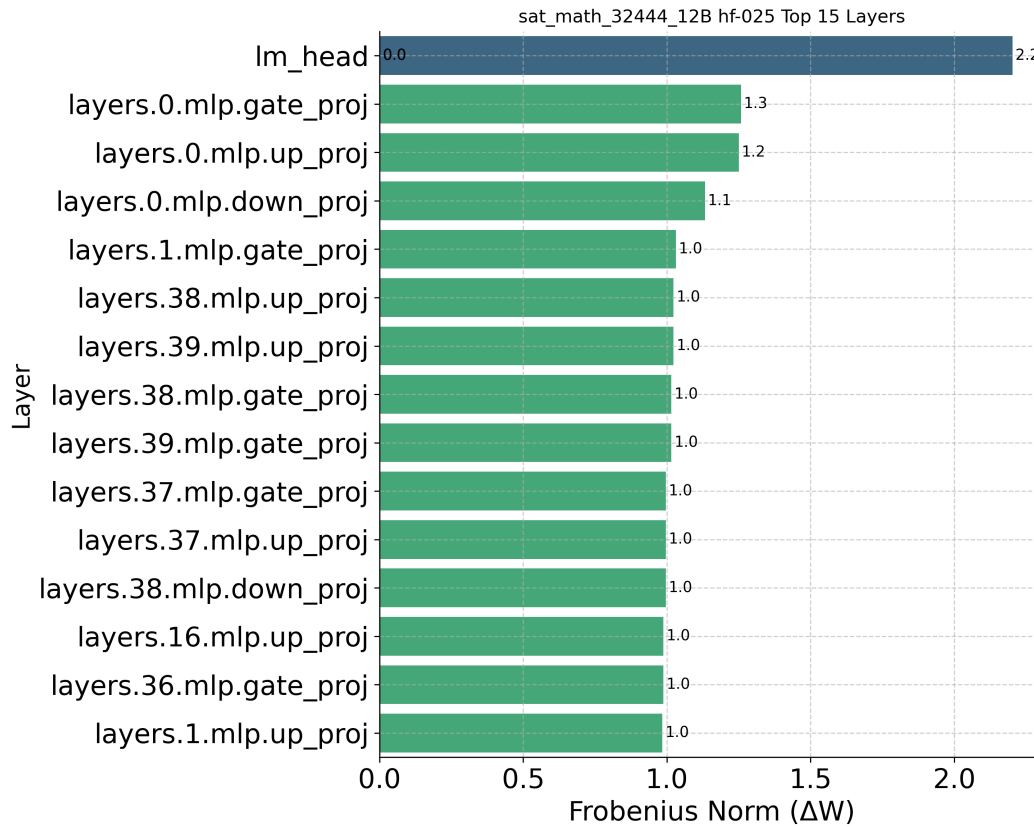


Figure 10: Ranking of Frobenius norm delta of layers of Llama-2-13b-chat after fine-tuning on SAT Math COT dataset, epoch 1

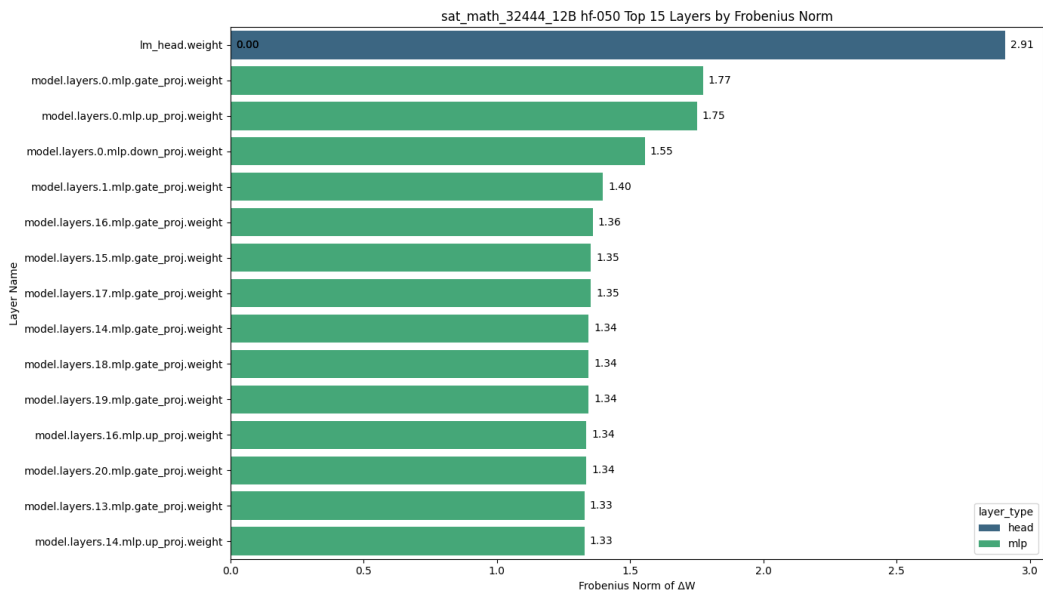


Figure 11: Ranking of Frobenius norm delta of layers of Llama-2-13b-chat after fine-tuning on SAT Math COT dataset, epoch 1